# X-ray and neutron reflectivity measurements of moisture transport through model multilayered barrier films for flexible displays

Bryan D. Vogt,[a)] Hae-Jeong Lee, Vivek M. Prabhu, Dean M. DeLongchamp, Eric K. Lin, and Wen-li Wu
*Polymers Division, National Institute of Standards and Technology, Gaithersburg, Maryland 20899*

Sushil K. Satija
*Center for Neutron Research, National Institute of Standards and Technology, Gaithersburg, Maryland 20899*

One encapsulation approach to extend the lifetime of flexible organic light-emitting diode (OLED) devices uses inorganic $Al_2O_3$-polymer multilayer barrier films. However, a recent theoretical examination of multilayer barriers indicated that the barriers should not be effective for OLED applications, despite empirical evidence of success. It was suggested that a long-lived transient process in the transport of water molecules through multilayer films is responsible for its practical success, but has not been directly observed experimentally. X-ray reflectivity (XR) and neutron reflectivity measurements are used to measure permeation rates and structural changes in model barrier films upon exposure to water vapor. A film consisting of a stack of an undercured organic and the typical inorganic phases was found to barely swell [$(7\pm5)$ Å] after an 11-d exposure to moisture [60 °C, 100% relative humidity (RH)]. Current measurements of ultralow moisture permeation assume that 10 d is sufficient for the equilibrium measurement, but XR data show that a stack of three dyad layers may require as many as 500 d ($>12\,000$ h) to reach equilibrium. Barriers with a high number of defects in the inorganic phase reached equilibrium after 6 d of exposure to moisture (60 °C, 100% RH). Over this time scale, water breakthrough at each layer can be observed from XR. Neutron reflectivity measurements with deuterated water show an accumulation of water near the aluminum oxide/polymer interface. This interface behaves similar to a desiccant, where the permeation of water through the barrier is retarded by the strong adsorption of water to aluminum oxide. This internal desiccant effect of the multilayered structure is clearly delineated and appears to be responsible for the long-term transient behavior of these barrier materials. [DOI: 10.1063/1.1923590]

## INTRODUCTION

The advances in the performance of organic electroluminescent (EL) materials over the past two decades have generated considerable interest in utilizing organic light-emitting devices (OLEDs) for full color displays.[1,2] OLEDs potentially provide several advantages including low power consumption, low cost, superior viewing angles, and the use of flexible substrates.[3] The primary shortcoming of most OLEDs is poor environmental stability that results in nonemissive regions upon extended exposure to ambient conditions. The degradation in performance is a result of the oxidation and delamination of the metal cathode[4] and the chemical reaction of the organic layer from exposure to moisture and oxygen. OLED lifetimes can be extended by orders of magnitude by device encapsulation.[5] Devices are generally sealed using a glass or metal lid held in place with epoxy. For additional protection, a desiccant is also incorporated within the package.[5] However, encapsulation with rigid barriers, such as glass, is incompatible with flexible OLED displays.

Plastic films are generally water permeable, leading to shorter lifetimes. The water-vapor permeation rate for most polymeric materials is between $10^1$ g/m$^2$/d and $10^{-1}$ g/m$^2$/d at ambient temperature. However, an *estimated* permeation rate of $5\times10^{-6}$ g/m$^2$/d or less is required to obtain a device lifetime of 10 000 h.[6] The plastic films must be modified to reduce their moisture (and oxygen) permeation rate(s). One additional difficulty in the production of a permeation barrier on the plastic substrate is the inherent roughness of commercially available plastic films, which often leads to holes and defects in the barrier.[7] Defects in the barrier layer tend to be the dominant factor controlling the moisture permeation.

Measuring and quantifying ultra-low permeation rates reliably and accurately is a major challenge. The most common permeation test is based upon the oxidation of calcium after moisture permeates through the barrier layer. The permeation rate is proportional to the rate of oxidation as monitored by changes in the optical transmittance of the Ca/CaO film.[8] More recently, a test has been developed based upon the detection of tritiated water by General Atomics. However, there are difficulties with both test techniques: the tritiated water test produces undesirable, highly contaminated radioactive waste and the Ca test suffers at times from edge sealing issues. Here, we introduce an approach to determine

a)Electronic mail: bryan.vogt@nist.gov

the permeation rate by measuring film swelling with x-ray and neutron reflectivity as a function of exposure time to humidity and temperature.

The elimination of all defects is probably necessary for a single-layer moisture barrier film as the permeation rate through the defect is generally much greater than $10^{-6}$ g/m$^2$/d. The *local* permeation rate through the film is the key factor to the OLED lifetime, not the average permeation rate. For large-area displays, the difficulties in obtaining a defect-free barrier have led to the investigation of alternative barrier materials, where a limited number of defects can be tolerated. One potential solution is the development of a hybrid organic-inorganic multilayer barrier coating.[9] In this work, the multilayer barrier studied is composed of polyacrylate films and inorganic oxide, deposited in alternating fashion. Each polymer-oxide layer pair is termed a "dyad."[10] This multilayered structure is an effective barrier material because the large permeation rate through defects in the inorganic layers is decoupled by the polymer layers, thus preventing a direct path for moisture through the barrier. OLEDs supported on the composite coated barrier films have been found to have extended lifetimes ($>3000$ h).[11] The same multilayer coating has been used to hermetically seal OLEDs, leading to highly flexible displays with extended lifetimes.[12]

Despite this empirical success, recent theoretical calculations indicate that the multilayer approach to moisture permeation barriers will not be effective if the observed permeation is an equilibrium process.[10] The success of the multilayer approach suggests that the low moisture permeation rate arises from long-term transient behavior. The equilibrium permeation is not an important value *if* the transient period is longer than the desired device lifetime.[10] The reflectivity based metrology developed here can provide details about the moisture permeation process through multilayer stacks. In this work, the polymer phase is undercured to ensure film swelling upon exposure to water (the swelling of highly cross-linked polymer might not be observable). The swelling of individual polymeric layers can be used to detect and follow the permeation process through the multilayer stack. Neutron reflectivity measurements with deuterated water are used to provide information of the water distribution within each dyad.

## EXPERIMENT

Model multilayer stacks were fabricated by alternate deposition of Al$_2$O$_3$ and polyacrylate onto silicon wafers in an integrated vacuum tool. The aluminum oxide is reactively sputtered using energetic plasma. Defects in the aluminum oxide were formed through the introduction of particulates during deposition. The polyacrylate layers are formed by flash evaporation of the monomer and subsequent ultraviolet (UV) radiation curing.[13] The degree of cross-linking of the polyacrylate is controlled through the curing conditions. By undercuring the polymer through decreasing the UV exposure dose, the degree of swelling upon exposure to moisture is enhanced.

The multilayer stacks examined here are three layers of alternating polyacrylate and Al$_2$O$_3$ (three dyads). Single-layer films were also included in this work to investigate the swelling of an individual polymer layer. These-single layer films consist of a thin Al$_2$O$_3$ coating on a silicon wafer, followed by application of approximately 0.5-$\mu$m-thick polyacrylate films. Two different cure conditions have been used, denoted as *a* and *b*. The difference in curing is that the lamp power used for cure *b* is 50% of cure *a*. All other cure conditions are kept constant. The thicknesses of the layers are similar to those used in high-performance multilayer barriers, although more dyads are typically used for barriers in devices.

The structure of the multilayer stacks was measured using specular x-ray reflectivity (XR). The reflectivity was collected in a $\theta/2\theta$ geometry using Cu K$_\alpha$ radiation focused by a bent crystal mirror into a four-bounce Ge (220) crystal monochromator. The reflected beam was further collimated through a three-bounce channel cut Ge (220) crystal prior to detection. The humidity at 60 °C was controlled inside an aluminum chamber with beryllium windows that was first evacuated (dry sample) and then backfilled with the equilibrium vapor from deionized water (MilliQ Millipore, Molsheim, France; 18.2 M$\Omega$ cm).

The water distribution in the single-layer films was determined with specular neutron reflectivity (NR) using the Center for Neutron Research NG-7 reflectometer at the National Institute of Standards and Technology (Gaithersburg, MD) utilizing cold neutrons with a wavelength ($\lambda$) $=4.768$ Å and wavelength spread ($\Delta\lambda/\lambda$)$=0.2$. NR is capable of probing the neutron scattering density at depths of up to several thousand angstrom, with an effective depth resolution of a few angstrom. The environmental control for the NR experiments was similar to the XR experiment, except that the sample chamber was equipped with silicon windows, heavy water (deuterium oxide; Aldrich, 99.9% pure) was used in place of H$_2$O, and the measurements were performed at ambient temperature.

## RESULTS AND DISCUSSION

The x-ray reflectivity (XR) profiles for single-layer films with different curing conditions are shown in Fig. 1. The reflectivity is shown as a function of the momentum-transfer vector $q$ where $q=4\pi \sin\theta/\lambda$, $\theta$ is the incident angle, and $\lambda$ is the radiation wavelength (1.54 Å for Cu K$_\alpha$). At the specular condition, XR probes the profile of the electron density perpendicular to the substrate. For these films, two frequencies are clearly visible; high-frequency oscillation corresponding to the total thickness as shown in Fig. 1 and low-frequency oscillation corresponding to the Al$_2$O$_3$ thickness as shown in Fig. 2. For cure *a* (100% lamp power), the polymer film swells from ($539.3\pm0.5$) nm to an equilibrium value of ($543.5\pm0.5$) nm (0.7% swelling) upon exposure to $\approx100$% relative humidity at 60 °C.[14] The thickness of the Al$_2$O$_3$ layer in this case is 9.6 nm. For cure *b* (50% lamp power), the polymer film swells from ($506.4\pm0.5$) nm to ($541.4\pm0.5$) nm (6.5% swelling) for the same conditions. In this case, the Al$_2$O$_3$ layer was 8.9 nm thick. Thus by controlling the curing conditions, the degree of polymer swelling
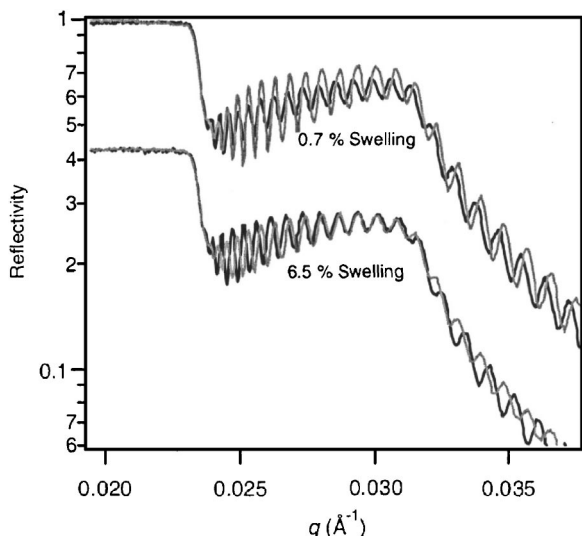
FIG. 1. X-ray reflectivity profiles for polyacrylate layer on $Al_2O_3$ with different curing conditions in vacuum (gray curve) and exposed to saturated $H_2O$ vapor at 60 °C (black curve). For cure *a* (top curves), the $Al_2O_3$ is 9.6 nm thick and the polymer swells from 539.3 to 543.5 nm. For cure *b* (bottom curves), the $Al_2O_3$ is 8.9 nm thick and the polymer swells from 506.4 to 541.4 nm. The reflectivity curves are offset for clarity.

upon exposure to moisture can be varied. The increased swelling in the most undercured sample (cure *b*) is a combination of the decrease in the cross-link density, which constrains the swelling, and the change in the chemistry of the film, as the cross-linkable moiety itself is hydrophilic but becomes hydrophobic after the cross-linking reaction.

Neutron reflectivity was used to monitor the water distribution within the same single-layer films. Isotopic labeling

by replacing protons with deuterium allows for the water ($D_2O$) to be distinguished from the polyacrylate with neutrons. The reflectivity profiles for the polyacrylate films on $Al_2O_3$ on silicon are shown in Fig. 2, both under vacuum and after exposure to saturated $D_2O$ vapor at ambient temperature ($22\pm3$ °C). Due to the wavelength spread and angular resolution of the neutron reflectometer, the total polymer film thickness cannot be resolved; however, the thickness of the aluminum oxide layer can be determined. In Fig. 2, the fringes in the reflectivity shift to lower $q$ upon exposure to $D_2O$ vapor for both cure conditions. This change in the reflectivity profile upon exposure to $D_2O$ vapor *appears* to be an increase in the $Al_2O_3$ layer thickness. However, water does not swell the $Al_2O_3$ as determined by XR (no shift in XR data). Because the neutron-scattering length density for $Al_2O_3$ is intermediate to that of the polyacrylate and $D_2O$, an accumulation of $D_2O$ at the interface that raises the local-scattering length density to a similar value as $Al_2O_3$ would also result in the observed shift in the reflectivity profiles. This shift is similar among the cure conditions despite the order-of-magnitude difference in water solubility. This accumulation of water at inorganic oxide/polymer interfaces is not unexpected and has been observed previously for several different systems.[15–19] Additionally, moisture accumulation at buried polymer/silicon oxide interface has been found to be relatively independent of the polymer, similar to the accumulation observed here for the single-layer films.[17]

The amount of $D_2O$ at the buried interface can be quantified by the change in the scattering length density after moisture exposure. The scattering length density profiles corresponding to the fit of the NR data are shown in Figs. 2(c)
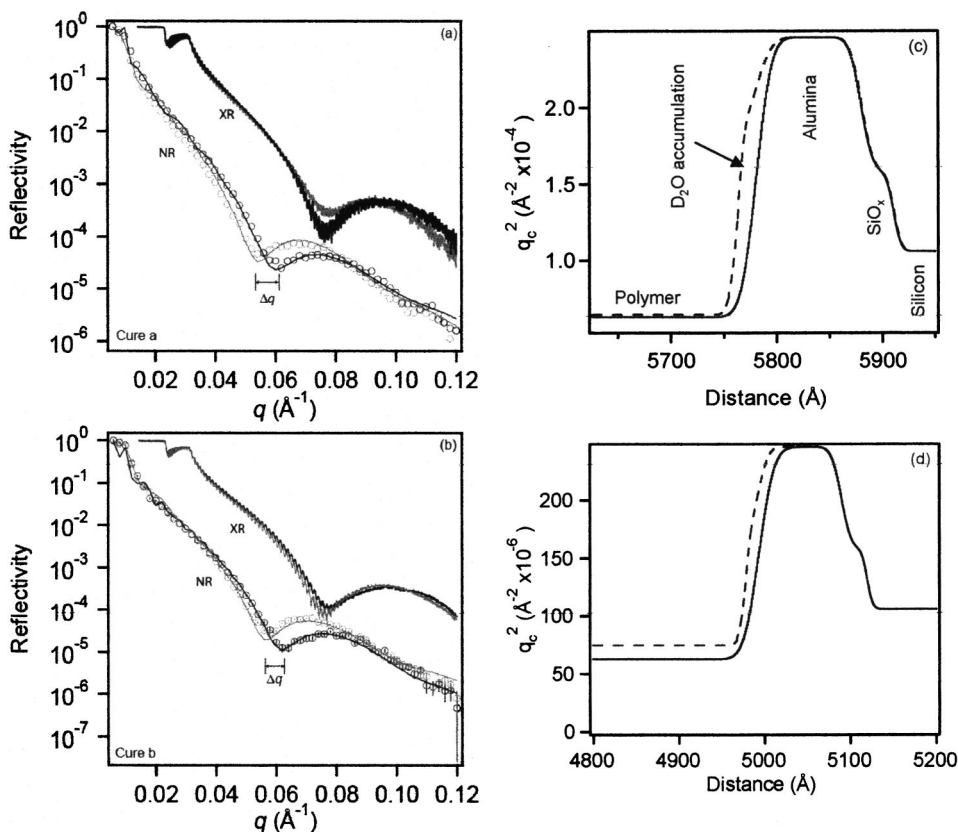


FIG. 2. Neutron and x-ray reflectivity profiles for polyacrylate layer on $Al_2O_3$ for (a) cure *a* and (b) cure *b* in vacuum (black curves) and exposed to saturated water vapor (gray curves). The minimum in neutron reflectivity shifts to lower $q$ upon exposure to $D_2O$ vapor, while no change is observed in the x-ray reflectivity minimum. Neutron-scattering length density profiles from the fit of the NR for (c) cure *a* and (d) cure *b*.

and 2(d). These density profiles are presented in terms of $q_c^2$ as a function of distance through the film. $q_c^2$ is a scattering length density, with dimensions Å$^{-2}$ and is proportional to the average atomic scattering length, $b$ ($q_c^2 = 16\pi Nb$). Calculating the water concentration in the film is made slightly more difficult by the surface roughness of the Al$_2$O$_3$. The Al$_2$O$_3$ is found to typically have roughness on the order of 25 Å, based upon assuming an error-function profile between the Al$_2$O$_3$ and the polymer or air. Coating the Al$_2$O$_3$ with the polyacrylate does not influence the roughness. This roughness is small in comparison to most glass substrates and comparable to high-quality float glass. However, it is significantly rougher than a silicon wafer and this roughness is on the same order as the thickness of the D$_2$O adsorbed at the buried interface. Thus, proper deconvolution of the Al$_2$O$_3$ from the D$_2$O swollen polymer phase is necessary to determine the water concentration. The concentration of the Al$_2$O$_3$ as a function of distance into the polyacrylate film (density profile) was determined for the dry state as follows:

$$\phi_{Al_2O_3}(x) = \frac{Q_c^2(x) - Q_{c,PA}^2}{Q_{c,Al_2O_3}^2 - Q_{c,PA}^2}, \tag{1}$$

where $Q_c^2(x)$ is the scattering length density at position $x$ in the film, $Q_{c,Al_2O_3}^2$ is the scattering length density of the pure Al$_2$O$_3$, and $Q_{c,PA}^2$ is the scattering length density of pure polyacrylate. With the assumption that the Al$_2$O$_3$ concentration (density) profile does not change upon D$_2$O exposure, the *water concentration profile* can then be calculated as

$$\phi_w(x) = \frac{Q_c^2(x) - (1 - \phi_{Al_2O_3}(x))Q_{c,PA}^2 - \phi_{Al_2O_3}(x) \cdot Q_{c,Al_2O_3}^2}{Q_{c,D_2O}^2 - (1 - \phi_{Al_2O_3}(x))Q_{c,PA}^2 - \phi_{Al_2O_3}(x) \cdot Q_{c,Al_2O_3}^2}, \tag{2}$$

where $\phi_w(x)$ is the water concentration at position $x$ in the film and $Q_{c,D_2O}^2$ is the scattering length density for pure D$_2$O. The calculated concentration profiles for both Al$_2$O$_3$ ($\phi_{Al_2O_3}$) and D$_2$O within the polymer phase ($\phi_w$) are shown in Fig. 3. The water concentration rapidly increases near the aluminum oxide surface for both cure conditions. The D$_2$O concentration profiles are approximately independent of the cure condition. There are several potential reasons for the differences observed in the water profiles, such as morphological differences in the Al$_2$O$_3$ surface, artifacts from the concentration determination which is a complex function of the fit scattering length density profiles [Eqs. (1) and (2)], instrumental resolution, or true differences based on different curing conditions. Nonetheless, it is clear that the water concentration profiles have two asymptotic values, irrespective of cure condition. The concentration increases to approximately 20% by volume water as the substrate is approached. The water concentration then decreases due to the presence of the solid Al$_2$O$_3$. The water profile is the total water concentration in the film including both the Al$_2$O$_3$ and the polymer. At the interface, the water concentration *within the polymer phase* approaches 40% by volume. The strength of the interaction between the Al$_2$O$_3$ and the water can be estimated from the rate of removal of water from the surface when exposed to ambient conditions (less humidity and lower temperature).
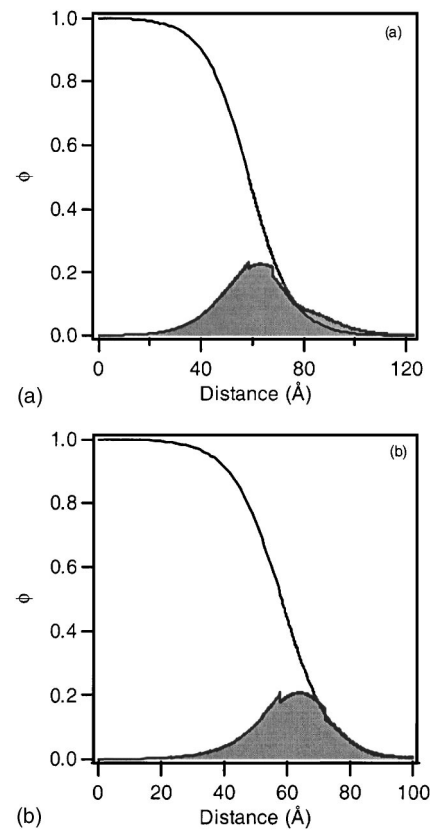


FIG. 3. Concentration profiles determined from neutron reflectivity for D$_2$O (shaded area) as a function of distance from pure Al$_2$O$_3$ interface for (a) cure *a* and (b) cure *b*. The Al$_2$O$_3$ density profile obtained from the dry film is shown by the solid line.

The width of the water excess near the interface decreases after ambient exposure for approximately 2 d, but the D$_2$O excess at the interface remains. This shows that the water is strongly bound to the interface and that deuterium from the surface water does not readily exchange with the protons from ambient H$_2$O. The work by Kent *et al.* has shown that water remains bound at a buried polymer/silicon oxide interface after months in vacuum.[16]

Next, to elucidate the influence of this interfacial accumulation, the structure of multilayer stacks and its evolution during moisture exposure was examined with x-ray reflectivity. Using curing *a*, a multilayer stack was created containing three dyads. The reflectivity profile from this stack is shown in Fig. 4(a) for a film prior to moisture exposure. The reflectivity now shows high oscillation fringes due to the total stack thickness and low oscillation fringes from the convoluted repeat thicknesses of the polymer/aluminum oxide layers. The reflectivity data are fit using a multilayer, least-squares-fitting algorithm[20] to extract the thickness and the real-space density profiles and are displayed in Fig. 4(b). The fit of the multilayer XR result is not optimal when the Al$_2$O$_3$/polymer interface is modeled as a hyperbolic tangent or error function. The sputtering of the inorganic Al$_2$O$_3$ on the polymer layers may result in an asymmetric interface profile, the form of which is not known. Nonetheless, the fit of the reflectivity curve in Fig. 2 does accurately follow the observed periodicities of the oscillations, such that the thickness of the layers is quantitatively captured by the fit. The
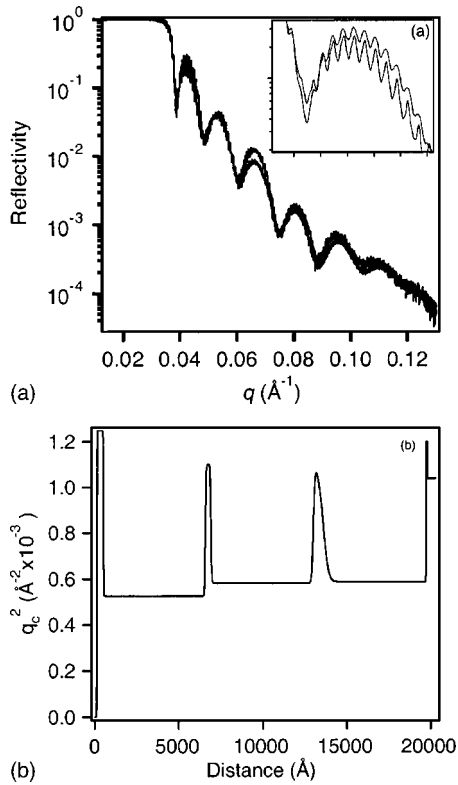
FIG. 4. (a) Reflectivity profile (thick line) for multilayer stack. Fit of the reflectivity profile to best represent the periodicities is shown by thin line. Inset shows fit of high-frequency fringes. (b) Scattering length density profile from fit of reflectivity periodicities.
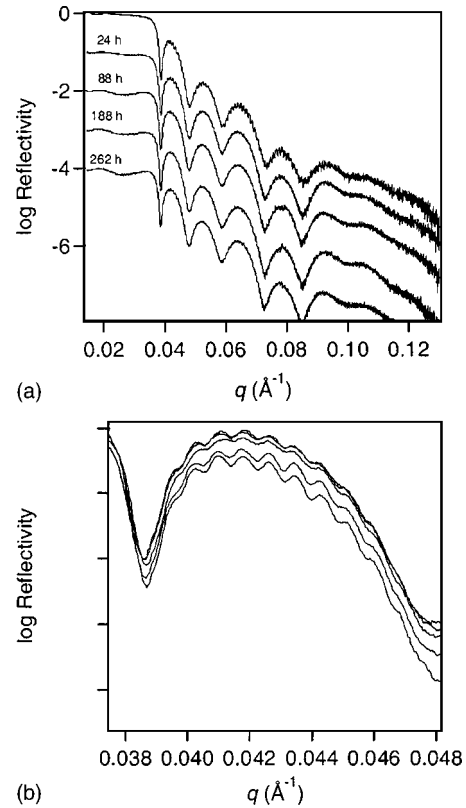


FIG. 5. X-ray reflectivity profiles for multilayer stack exposed to saturated $H_2O$ vapor at 60 °C for different exposure times. The whole reflectivity curves (a) as well as a limited range illustrating the high-frequency oscillations (b) show limited change over the course of 11 d. The reflectivity profiles are offset for clarity.

density profile in Fig. 4(b) illustrates the structure of the multilayers but is not quantitative in its description of the interfaces and the absolute value of the scattering length densities. These density profiles are presented in terms of $Q_c^2$ as a function of distance through the film. For the XR data in Fig. 4, the angle $\theta_c$ corresponding to $Q_c^2$ is proportional to the electron density of the film $\rho_e$ (and thus the mass density) through the relation $\theta_c = \lambda(\rho_e r_e/\pi)^{0.5}$, where $r_e$ is the classical radius of an electron. The density profile begins in vacuum with a scattering length density of zero and then increases to $Q_c^2$ of $Al_2O_3$ as the distance axis is increased. The thickness of each $Al_2O_3$ layer is approximately 40 nm, followed by approximately 500 nm of polyacrylate with cure condition $a$. There are three repeat layers (dyads), as seen in Fig. 4(b). After the alternating layers, a thin coating of $Al_2O_3$, approximately 10 nm thick, is present before the silicon substrate. Two distinct oscillation frequencies were present in the observed XR result, with the low frequency corresponding to the thickness of $Al_2O_3$ and the high frequency corresponding to the total layer thickness. Small changes in the structure shift the minima locations significantly for both frequencies, so that changes to the structure of the multilayer stack during exposure to moisture can be determined quantitatively. The density profile shown in Fig. 4(b) is only qualitative as the data were not fitted well at all $q$. However, the total thickness of the film can be extracted quantitatively by the frequency of the reflectivity.

The reflectivity profiles from a three-dyad multilayer stack with cure $a$, exposed to moisture at 60 °C and ≈100%

relative humidity, are shown in Fig. 5 as a function of exposure time. The changes to the reflectivity profile over the course of 11 d are small with a total thickness increase of $(7\pm5)$ Å. The equilibrium swelling of each individual polymer layer is determined to be approximately 30 Å, which suggests that 90 Å of swelling would be observed. In general, elevated temperature and relative humidity are used to accelerate the permeation test to a time period of 10 d. Clearly, for the multilayered "barrier" examined here, 10 d is not sufficient to reach equilibrium, as was suggested by the data of Graff *et al.*[10] Although the change in thickness is quite small, the time required to reach equilibrium can be roughly estimated. Assuming the swelling rate remains constant through all the layers, at least 85 d will be required to reach equilibrium. These estimates are in line with calculated lag times for three dyads.[10] However, it is clear that the typical exposure time for permeation tests is not enough to reach equilibrium. The moisture absorption process into glassy polymers has been a subject of much interest over the past 60 years.[21–24] It has been postulated that moisture absorption within a glassy polymer first occurs within voids/free volume, then within the polymer as the equilibrium concentration is reached. For these films, the observed transient time could result from the filling of the voids within the polymer film before reaching the apparent constant permeation rate after the polymer phase reaches equilibrium.

Since the moisture permeation through inorganic films in general is dominated by defects, the polymeric layers should
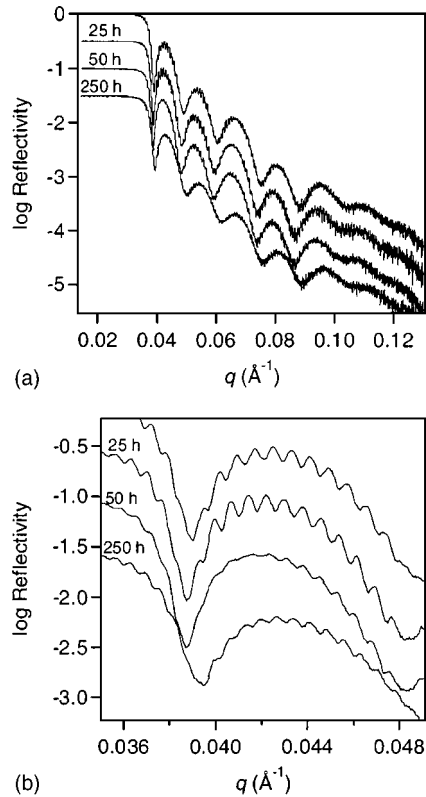
(a)



(b)

FIG. 6. X-ray reflectivity profiles for multilayer stack with defects in inorganic layers exposed to saturated $H_2O$ vapor at 60 °C for different exposure times. The whole reflectivity curves (a) as well as a limited range illustrating the high-frequency oscillations (b) show the change in both the repeat thickness within the stack and the increase in total thickness upon moisture exposure. The reflectivity profiles are offset for clarity.
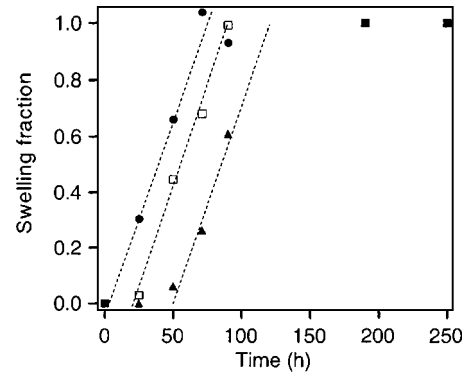


FIG. 7. Swelling of each polymer layer as determined by fitting periodicities of the XR from multilayered stack with defects. The top layer (•) swells first, then the middle layer (□), and finally the bottom layer (▲). The delay time to begin swelling increases as water progresses through the film. The lines are drawn as an aid to the reader.

reach equilibrium in a shorter period if a significant number of defects were introduced to each of the inorganic layers in the multilayer stack. To elucidate the moisture transport through a multilayer film in a reasonable exposure time, another three-layer dyad using cure *a* was synthesized with $Al_2O_3$ layers that contain a significant number of defects. We observe a significantly greater film swelling in this film with defects, in comparison to the previous sample. All three polymer layers reach equilibrium after 200 h of exposure to ≈100% relative humidity at 60 °C. The reflectivity curves at several exposure times are shown in Fig. 6. A comparison of the reflectivity curves in Figs. 5 and 6 reveal significantly more changes in the reflectivity profiles for the stack with defect-filled $Al_2O_3$ layers. The total film thickness increases, as is clear from the shift in fringes to lower $q$ after 25 h [Fig. 6(b)]. The swelling of the film is determined by fitting to the periodicities. The alumina layers are assumed to remain constant; only the thickness of the polymeric layers is allowed to vary to fit the observed oscillation frequencies. The swelling of each polymer layer after 250 h exposure is slightly different (0.7% to 1.1%) between layers, but is similar to the swelling observed for the single-layer film (0.7%). This difference between layers may be due to slight variations in the curing, but no significant or systematic deviation in the swelling is observed (and hence the degree of curing). From fits of the reflectivity profiles, the swelling of each individual polymer layer can be monitored as a function of time as

shown in Fig. 7. Once a layer begins to swell, the swelling rate appears to be constant (approximately 17 Å/d) for each layer. This correlates to a permeation rate of $1.7 \times 10^{-3}$ g/m$^2$/d, assuming that the density of the absorbed water is 1 g/cm$^3$. This is a reasonable permeation rate for an $Al_2O_3$ barrier with defects. As a comparison for the original sample examined (Fig. 3), the permeation rate was less than $10^{-5}$ g/m$^2$/d (60 °C, 100% relative humidity) based upon the same assumption. The time delay for the initiation of swelling in each layer appears to increase for each subsequent layer (Fig. 7). Since the moisture accumulation (permeation) rate through the different layers is nearly constant, this increase in the transient region is believed to be related to the intrinsic properties of the barrier materials.

Water accumulation at the $Al_2O_3$/polymer interface has significant implications in the permeation of water through the multilayered barrier films. First and foremost, the accumulation of water on inorganic oxides has long been used within the encapsulated device, but this is considered as a desiccant (e.g., CaO).[5] For the case of these multilayered structures, the desiccant is built into the barrier itself. Once moisture reaches the polymer phase, there are many potential binding sites that limit further permeation of moisture into the device. As water diffuses through defects in the alumina layer and into the polymer layer, it adsorbs to the inorganic oxide when it approaches a surface. As long as the defects between layers are not correlated, the oxide interfaces should initially decrease the quantity of water available to diffuse into the next barrier layer or the OLED due to the surface adsorption. This leads to an apparent decrease in the permeation rate through the barrier until the $Al_2O_3$ surfaces are saturated, at which point the equilibrium permeation for the barrier would be obtained. If the time to saturate the surfaces is greater than the desired device lifetime, then the equilibrium permeation is irrelevant. Although the moisture accumulation was demonstrated at the interface when the polymer film was applied to the $Al_2O_3$ surface, identical accumulation at the interface when $Al_2O_3$ is sputtered onto the polymer may not necessarily occur. Based upon the previous characterizations of polymer/aluminum interfaces,[25,26] it is probable that the $Al_2O_3$ reacts with the polyacrylate.

This would be similar, in effect, to the treatment of the $Al_2O_3$ surface with hydrophobic moieties, which has been shown to decrease the concentration of moisture that accumulates at the buried interface.[15,18] Nonetheless, the side where the polyacrylate is polymerized will adsorb moisture. This desiccant effect of the $Al_2O_3$ shown here is a potential source of the long-lived transient behavior of multilayer barrier materials previously discussed by Graff *et al.* in terms of an extremely long effective path length.[10]

## CONCLUSIONS

Recently, the theoretical examination of inorganic-organic multilayer barriers indicated that the barriers should not be effective for OLED applications, despite the wealth of experimental evidence from permeation test results suggesting otherwise. It was speculated that the source of this discrepancy is a long-lived transient process in the transport of water molecules through multilayer films. The transient behavior of model multilayer films was examined with x-ray and neutron reflectivity. A film consisting of a stack of an undercured organic and the typical inorganic phases was found to barely swell over the course of 11 d $[(7\pm5)$ Å$]$ when exposed to moisture (60 °C, 100% RH). At equilibrium, this film is expected to swell in excess of 90 Å, and each individual organic layer should swell to 30 Å. Current metrologies for the measurement of ultralow moisture permeation assume that 10 d is sufficient for the equilibrium measurement, but clearly this is not the case for these multilayered barriers. It is estimated that as many as 500 d ( >12 000 h) may be required for a three-layer barrier to equilibrate. In an attempt to measure the transport through these films on a reasonable time scale, barriers with atypically high number of defects in the inorganic phase were produced. These films reached equilibrium after 6 d of exposure to moisture [60 °C, 100% relative humidity (RH)]. The water breakthrough of each layer can be observed from the reflectivity data. The delay time to breakthrough increases with each layer, thus it appears that there may be a synergistic effect of adding layers. Through the deuterium labeling of the water, an accumulation of water near the aluminum oxide/polymer interface was observed. This interface behaves similar to a desiccant, with further water permeation into the barrier (or active matrix) retarded by the strong adsorption to the aluminum oxide. The adsorbed water does not readily leave the oxide surface. This internal desiccant effect of the multilayered structure appears to be responsible for the long-term transient behavior of these barrier materials.

[1]R. H. Friend *et al.*, Nature (London) **397**, 121 (1999).
[2]D. Kalinowski, J. Phys. D **32**, R179 (2004).
[3]S. H. Ju *et al.*, SID Int. Symp. Digest Tech. Papers **33**, 1096 (2002).
[4]S. F. Lim, W. Wang, and S. J. Chua, Adv. Funct. Mater. **12**, 513 (2002).
[5]P. E. Burrows, V. Bulovic, S. R. Forrest, L. S. Sapochak, D. M. Mccarty, and M. E. Thompson, Appl. Phys. Lett. **65**, 2922 (1994).
[6]P. E. Burrows *et al.*, Displays **22**, 65 (2001).
[7]H. Chatham, Surf. Coat. Technol. **78**, 1 (1996).
[8]G. Nisato, P. C. P Bouten, P. J. Slinkkerveer, W. D. Bennet, G. L. Graff, N. Rutherford, and L. Wiese, *21st International Asia Display/8th International Display Workshop, Nagoya, Japan, 16–19 October 2001.*
[9]P. E. Burrows *et al.*, Proc. SPIE **4105**, 75 (2000).
[10]G. L. Graff, R. E. Williford, and P. E. Burrows, J. Appl. Phys. **96**, 1840 (2004).
[11]M. S. Weaver *et al.*, Appl. Phys. Lett. **81**, 2929 (2002).
[12]A. B. Chwang *et al.*, Appl. Phys. Lett. **83**, 413 (2003).
[13]J. D. Affinito, M. E. Gross, P. A. Mounier, M. K. Shi, and G. L. Graff, J. Vac. Sci. Technol. A **17**, 1974 (1999).
[14]The data throughout the manuscript and the figures are presented along with the standard uncertainty ($\pm$) involved in the measurement based on one standard deviation.
[15]M. S. Kent, G. S. Smith, S. M. Baker, A. Nyitray, J. Browning, and G. Moore, J. Mater. Sci. **31**, 927 (1996).
[16]M. S. Kent, W. F. McNamara, D. B. Fein, L. A. Domeier, and A. P. Y. Wong, J. Adhes. **69**, 121 (1999).
[17]B. D. Vogt *et al.*, Langmuir **20**, 5285 (2004).
[18]B. D. Vogt *et al.*, J. Microlithogr., Microfabr., Microsyst. **4**, 013003 (2005).
[19]W. L. Wu, W. J. Orts, C. J. Majkrzak, and D. L. Hunston, Polym. Eng. Sci. **35**, 1000 (1995).
[20]J. F. Ankner and C. F. Maikrzak, Proc. SPIE **1738**, 260 (1992).
[21]J. A. Barrie, *Water in Polymers*, edited by J. Crank and G. S. Park (Academic, London, 1968), Chap. 8, pp. 259–314.
[22]R. Blahnik, Prog. Org. Coat. **11**, 353 (1983).
[23]P. M. Hauser and A. D. McLaren, Ind. Eng. Chem. **40**, 112 (1948).
[24]G. K. van der Wel and O. C. G. Adan, Prog. Org. Coat. **37**, 1 (1999).
[25]M. Bou, J. M. Martin, T. L. Mogne, and T. L. Vovelle, Appl. Surf. Sci. **47**, 149 (1991).
[26]P. Stoyanov, S. Akhter, and J. M. White, Surf. Interface Anal. **15**, 509 (1990).